Two-Dimensional Phase Unwrapping Based on Selective Smoothing and Inconsistency Correction

Daichi KITAHARA† Isao YAMADA†
†Department of Communications and Computer Engineering, Tokyo Institute of Technology

Abstract Two-dimensional (2D) phase unwrapping is an reconstruction problem of a continuous phase, over a 2D domain, from its wrapped samples. 2D phase unwrapping is important in applications such as terrain height estimation by interferometric synthetic aperture radar and water/fat separation in magnetic resonance imaging. In this paper, for noisy data, we propose a novel 2D phase unwrapping algorithm. The proposed algorithm first computes, via convex optimization, a rough estimate of the continuous phase by promoting smoothness for unreliable neighboring pairs of samples. Then the proposed algorithm corrects the inconsistency between the rough estimate and the observed wrapped samples while keeping a certain level of smoothness. Numerical simulations for terrain height estimation demonstrate the effectiveness of the proposed algorithm.

1 Introduction

Two-dimensional (2D) phase unwrapping [1], [2] is a reconstruction problem of an unknown continuous phase function $\Theta : \mathbb{R}^2 \to \mathbb{R}$ from its noisy wrapped samples

$$\Theta^W := W(\Theta + \nu) \in (-\pi, \pi] \tag{1}$$

observed at $(x_i, y_j) \in \mathbb{R}^2$ s.t. $x_{i+1} - x_i = h_x > 0$ ($i = 0, 1, \ldots, n-1$) and $y_{j+1} - y_j = h_y > 0$ ($j = 0, 1, \ldots, m-1$), where ν is additive noise and $W : \mathbb{R} \to (-\pi, \pi]$ is the *wrapping operator* defined by

$$\forall \vartheta \in \mathbb{R}\ \exists \eta \in \mathbb{Z} \quad \vartheta = W(\vartheta) + 2\pi\eta \text{ and } W(\vartheta) \in (-\pi, \pi].$$

The continuous phase $\Theta_{i,j} := \Theta(x_i, y_j)$ and its noisy wrapped sample $\Theta^W_{i,j} := \Theta^W(x_i, y_j)$ are respectively called the *unwrapped phase* and the *wrapped phase*. 2D phase unwrapping is important for signal and image processing applications such as *terrain height estimation* (see Section 3.1) and *landslide identification* by interferometric synthetic aperture radar (InSAR) [3]–[9], *seafloor depth estimation* by interferometric synthetic aperture sonar (InSAS) [10]–[13], *3D shape measurement* by fringe projection [14]–[17] or X-ray [18]–[21], and *water/fat separation* in magnetic resonance imaging (MRI) [22]–[25].

Most 2D phase unwrapping algorithms assume that many unwrapped phase differences $\Theta_{i+1,j} - \Theta_{i,j}$ and $\Theta_{i,j+1} - \Theta_{i,j}$ are within $\pm\pi$, and these algorithms have been designed to suppress a certain function $J : \mathbb{R}^{(m+1)(n+1)} \to \mathbb{R}_+$ measuring the unwrapped phase differences as

$$J(\boldsymbol{\Theta}) := \sum_{i=0}^{n-1}\sum_{j=0}^{m} w^x_{i,j} \left|\Theta_{i+1,j} - \Theta_{i,j} - W\big(\Theta^W_{i+1,j} - \Theta^W_{i,j}\big)\right|^p + \sum_{i=0}^{n}\sum_{j=0}^{m-1} w^y_{i,j} \left|\Theta_{i,j+1} - \Theta_{i,j} - W\big(\Theta^W_{i,j+1} - \Theta^W_{i,j}\big)\right|^p, \tag{2}$$

where $\boldsymbol{\Theta} := \mathrm{vec}(\Theta_{i,j})_{j=0,1,\ldots,m}^{i=0,1,\ldots,n} \in \mathbb{R}^{(m+1)(n+1)}$, $w^x_{i,j} > 0$, $w^y_{i,j} > 0$ and $p > 0$. For example, branch cut (BC) algorithm [5] and minimum spanning tree (MST) algorithm [26] employ $p \to +0$, minimum cost flow (MCF) algorithm [27] employs $p = 1$, and least squares (LS) algorithm [28] employs $p = 2$. Such a specification of J is introduced on the basis of a simple property that, under the assumption $\nu = 0$, $\Delta\Theta = W(\Delta\Theta^W)$ holds if and only if $|\Delta\Theta| < 0$, where $\Delta\Theta$ and $\Delta\Theta^W$ respectively denote the unwrapped and wrapped phase differences.

BC, MST and MCF algorithms try to find a minimizer of J under the condition

$$\forall i, j\ \exists \eta_{i,j} \in \mathbb{Z} \quad \Theta_{i,j} = \Theta^W_{i,j} + 2\pi\eta_{i,j}. \tag{3}$$

This type of optimization problem is combinatorial and intractable due to condition (3). In order to solve this problem, these algorithms use an elegant technique developed originally for network flow in graph theory [2], [26]. In this approach, if the observed wrapped phase has only small noise and the unwrapped phase difference is sufficiently small with respect to sampling interval, we can construct a very good estimate. However, otherwise, condition (3) is violated due to noise ν in (1), and the minimizer of J is hard to compute due to condition (3).

LS algorithm directly computes a minimizer $\boldsymbol{\Theta}^*$ of J without requiring condition (3). In this approach, even if the observed wrapped phase is noisy, $\boldsymbol{\Theta}^*$ can be obtained. However since condition (3) is not guaranteed, consistency between Θ^* and Θ^W, e.g., $W(\Theta^*_{i,j}) \approx \Theta^W_{i,j}$ and $W(\Delta\Theta^*) \approx W(\Delta\Theta^W)$, may possibly be lost.

In this paper, we propose a novel 2D phase unwrapping algorithm for noisy data. We assume that the shape of the unwrapped phase is smooth. Here the word "smooth" means that the absolute value of the second-order difference, i.e., $|\Delta^2\Theta|$, is small over $\mathbb{R}^2$. Therefore we newly design a convex cost function $\widetilde{J} : \mathbb{R}^{(m+1)(n+1)} \to \mathbb{R}_+$ to promote $\Delta\Theta \approx W(\Delta\Theta^W)$ for only reliable neighboring pairs as well as to enhance smoothness for other neighboring pairs. As a result, $\widetilde{J}$ is defined as the sum of (2) and the square of the weighted ℓ_2-norm of the second-order difference, where the values of the weights can be determined by only the wrapped phase information. Then we find a minimizer of $\widetilde{J}$ without condition (3) by alternating direction method of multipliers (ADMM) [29]. Finally, we correct the inconsistency between the minimizer and condition (3) while keeping a certain level of smoothness, and this corrected version is used as an estimate of the unwrapped phase. Simulation for terrain height estimation by InSAR demonstrates the effectiveness of the proposed algorithm.

Notation Let $\mathbb{Z}$, $\mathbb{R}$, $\mathbb{R}_+$ and $\mathbb{R}_{++}$ be respectively the set of all integers, real numbers, nonnegative real numbers and positive real numbers. A boldface letter expresses a vector or a matrix depending on the situation. For any vector $\boldsymbol{x} \in \mathbb{R}^n$ and matrix $\boldsymbol{X} \in \mathbb{R}^{n\times m}$, $[\boldsymbol{x}]_i$ and $[\boldsymbol{X}]_{i,j}$ respectively denote the ith component of $\boldsymbol{x}$ and the (i,j) entry of $\boldsymbol{X}$. For $p \geq 1$ and $\boldsymbol{w} \in \mathbb{R}^n_{++}$, the ℓ_p-norm and the weighted ℓ_p-norm of $\boldsymbol{x} \in \mathbb{R}^n$ are respectively defined as $\|\boldsymbol{x}\|_p := \sqrt[p]{\sum_{i=1}^n |[\boldsymbol{x}]_i|^p}$ and $\|\boldsymbol{x}\|_{p,\boldsymbol{w}} := \sqrt[p]{\sum_{i=1}^n [\boldsymbol{w}]_i |[\boldsymbol{x}]_i|^p}$.

2 Proposed 2D Phase Unwrapping by Selective Smoothing and Inconsistency Correction

We assume that the true unwrapped phase Θ is smooth. Here the word "smooth" means that the absolute value of the second-order difference, i.e., $|\Delta^2\Theta|$, is small over $\mathbb{R}^2$. Therefore we reconstruct Θ by enhancing smoothness for noisy area. The main idea of the proposed 2D phase unwrapping algorithm is divided into the following two steps.

Step 1. Compute a rough estimate Θ^* of Θ via convex optimization to promote $\Delta\Theta^* \approx W(\Delta\Theta^W)$ for only reliable neighboring pairs as well as to enhance smoothness for other neighboring pairs.

Step 2. Construct a modified version $\widehat{\Theta}$ of Θ^* by correction of inconsistency between $\Theta^*_{i,j}$ and $\Theta^W_{i,j}$ while keeping the smoothness of $\Theta^*_{i,j}$.

2.1 Selective Smoothing by Convex Optimization (Step 1)

2.1.1 Unreliable Neighboring Pair Type 1

Suppose $\Delta\Theta \in (-\pi, \pi]$ for all neighboring pairs. In this simple situation, $W(\Delta\Theta^W) = \Delta\Theta$ holds if additive noise is negligible. However, if there exists a neighboring pair such that $|\Delta\Theta| \approx \pi$, then even very small additive noise can drastically influence $W(\Delta\Theta^W)$, e.g., $W(\Delta\Theta^W) \approx \Delta\Theta \pm 2\pi$ in the worst case scenario. This can be verified as seen in an example: $\Delta\Theta = \pm 0.95\pi$ and $\Delta\nu = \pm 0.1\pi$ result in $W(\Delta\Theta^W) = W(\Delta\Theta + \Delta\nu) = W(\pm 1.05\pi) = \mp 0.95\pi = \Delta\Theta \mp 1.9\pi$. This observation suggests that

$$W\big(\Delta\Theta^W\big) \text{ is not reliable if } \big|W\big(\Delta\Theta^W\big)\big| \approx \pi.$$

2.1.2 Unreliable Neighboring Pair Type 2

In the neighborhood of *residue* [5], there are at least one neighboring pair s.t. $\Delta\Theta \neq W(\Delta\Theta^W)$. Moreover, residues are often produced due to the influence of additive noise. This observation suggests that

$$W\big(\Delta\Theta^W_{\boldsymbol{i}}\big) \text{ is not reliable in region having many residues.}$$

2.1.3 Unreliable Neighboring Pair Type 3

If amplitude information is available other than wrapped phase information, the amplitude can be used to detect unreliable neighboring pairs. Indeed the wrapped phase is not reliable due to the influence of additive noise in the area where the amplitude is very small.

2.1.4 Convex Optimization for Selective Smoothing

To enhance the smoothness of Θ^* for unreliable neighboring pairs of Type 1 or Type 2 (or Type 3 if amplitude information is available) as well as to promote $\Delta\Theta^* \approx W(\Delta\Theta^W)$ for other neighboring pairs, we find a minimizer $\boldsymbol{\Theta}^*$ of the following convex function:

$$\begin{aligned}
\widetilde{J}(\boldsymbol{\Theta}) :=& \sum_{i=0}^{n-1}\sum_{j=0}^{m} w^x_{i,j}\big|\Theta_{i+1,j} - \Theta_{i,j} - W\big(\Theta^W_{i+1,j} - \Theta^W_{i,j}\big)\big| \\
&+ \sum_{i=0}^{n}\sum_{j=0}^{m-1} w^y_{i,j}\big|\Theta_{i,j+1} - \Theta_{i,j} - W\big(\Theta^W_{i,j+1} - \Theta^W_{i,j}\big)\big| \\
&+ \sum_{i=0}^{n-2}\sum_{j=0}^{m} w^{xx}_{i,j}|\Theta_{i+2,j} - 2\Theta_{i+1,j} + \Theta_{i,j}|^2 \\
&+ \sum_{i=0}^{n-1}\sum_{j=0}^{m-1} w^{xy}_{i,j}|\Theta_{i+1,j+1} - \Theta_{i+1,j} - \Theta_{i,j+1} + \Theta_{i,j}|^2 \\
&+ \sum_{i=0}^{n}\sum_{j=0}^{m-2} w^{yy}_{i,j}|\Theta_{i,j+2} - 2\Theta_{i,j+1} + \Theta_{i,j}|^2 + \epsilon\|\boldsymbol{\Theta}\|^2, \quad (4)
\end{aligned}$$

where we assign small values to $w^x_{i,j} > 0$ and $w^y_{i,j} > 0$ if $|W(\Theta^W_{i+1,j} - \Theta^W_{i,j})| \approx \pi$ and $|W(\Theta^W_{i,j+1} - \Theta^W_{i,j})| \approx \pi$, respectively, we assign large values to $w^{xx}_{i,j} > 0$, $w^{xy}_{i,j} > 0$ and $w^{yy}_{i,j} > 0$ if there are many residues in the vicinity of (x_i, y_j) (see such examples in Section 3.2), and $\epsilon\|\boldsymbol{\Theta}\|^2$ $(0 < \varepsilon \ll 1)$ is introduced for the regularization.

The expression of $\widetilde{J}(\boldsymbol{\Theta})$ is simplified as

$$\begin{aligned}
\widetilde{J}(\boldsymbol{\Theta}) =& \|\boldsymbol{D}_x\boldsymbol{\Theta} - \boldsymbol{\delta}_x\|_{1,\boldsymbol{w}_x} + \|\boldsymbol{D}_y\boldsymbol{\Theta} - \boldsymbol{\delta}_y\|_{1,\boldsymbol{w}_y} \\
&+ \|\boldsymbol{D}_{xx}\boldsymbol{\Theta}\|^2_{2,\boldsymbol{w}_{xx}} + \|\boldsymbol{D}_{xy}\boldsymbol{\Theta}\|^2_{2,\boldsymbol{w}_{xy}} + \|\boldsymbol{D}_{yy}\boldsymbol{\Theta}\|^2_{2,\boldsymbol{w}_{yy}} + \epsilon\|\boldsymbol{\Theta}\|^2,
\end{aligned}$$

where $\boldsymbol{D}_x$, $\boldsymbol{D}_y$, $\boldsymbol{D}_{xx}$, $\boldsymbol{D}_{xy}$ and $\boldsymbol{D}_{yy}$ are matrices satisfying

$$\left.\begin{aligned}
\boldsymbol{D}_x\boldsymbol{\Theta} &= \mathrm{vec}(\Theta_{i+1,j} - \Theta_{i,j}) \\
\boldsymbol{D}_y\boldsymbol{\Theta} &= \mathrm{vec}(\Theta_{i,j+1} - \Theta_{i,j}) \\
\boldsymbol{D}_{xx}\boldsymbol{\Theta} &= \mathrm{vec}(\Theta_{i+2,j} - 2\Theta_{i+1,j} + \Theta_{i,j}) \\
\boldsymbol{D}_{xy}\boldsymbol{\Theta} &= \mathrm{vec}(\Theta_{i+1,j+1} - \Theta_{i+1,j} - \Theta_{i,j+1} + \Theta_{i,j}) \\
\boldsymbol{D}_{yy}\boldsymbol{\Theta} &= \mathrm{vec}(\Theta_{i,j+2} - 2\Theta_{i,j+1} + \Theta_{i,j})
\end{aligned}\right\},$$

$\boldsymbol{\delta}_x = \mathrm{vec}(W(\Theta^W_{i+1,j} - \Theta^W_{i,j}))$, $\boldsymbol{\delta}_y = \mathrm{vec}(W(\Theta^W_{i,j+1} - \Theta^W_{i,j}))$, $\boldsymbol{w}_x = \mathrm{vec}(w^x_{i,j})$, $\boldsymbol{w}_y = \mathrm{vec}(w^y_{i,j})$, $\boldsymbol{w}_{xx} = \mathrm{vec}(w^{xx}_{i,j})$, $\boldsymbol{w}_{xy} = \mathrm{vec}(w^{xy}_{i,j})$, and $\boldsymbol{w}_{yy} = \mathrm{vec}(w^{yy}_{i,j})$. To solve this convex optimization problem, we use alternating direction method of multipliers (ADMM) [29]. A minimizer $\boldsymbol{\Theta}^*$ of $\widetilde{J}$ is approximated iteratively by ADMM as

$$\left|\begin{aligned}
\boldsymbol{\Theta}_{i+1} &= (\boldsymbol{D}_1^T\boldsymbol{D}_1 + 2\gamma(\boldsymbol{D}_2^T\boldsymbol{W}_2\boldsymbol{D}_2 + \varepsilon\boldsymbol{I}))^{-1}\boldsymbol{D}_1^T(\boldsymbol{z}_i - \boldsymbol{\xi}_i) \\
\boldsymbol{z}_{i+1} &= \mathcal{U}(\boldsymbol{D}_1\boldsymbol{\Theta}_{i+1} + \boldsymbol{\xi}_i) \\
\boldsymbol{\xi}_{i+1} &= \boldsymbol{\xi}_i + \boldsymbol{D}_1\boldsymbol{\Theta}_{i+1} - \boldsymbol{z}_{i+1}
\end{aligned}\right.$$

where $\gamma > 0$, $\boldsymbol{D}_1 = (\boldsymbol{D}_x^T, \boldsymbol{D}_y^T)^T$, $\boldsymbol{D}_2 = (\boldsymbol{D}_{xx}^T, \boldsymbol{D}_{xy}^T, \boldsymbol{D}_{yy}^T)^T$, $\boldsymbol{W}_2$ is a diagonal matrix constructed by using $\boldsymbol{w}_2 = (\boldsymbol{w}_{xx}^T, \boldsymbol{w}_{xy}^T, \boldsymbol{w}_{yy}^T)^T$ as $[\boldsymbol{W}_2]_{i,i} = [\boldsymbol{w}_2]_i$, $\boldsymbol{I}$ is the identity matrix, and the operator $\mathcal{U}$ is defined, with the use of $\boldsymbol{w}_1 = (\boldsymbol{w}_x^T, \boldsymbol{w}_y^T)^T$ and $\boldsymbol{\delta} = (\boldsymbol{\delta}_x^T, \boldsymbol{\delta}_y^T)^T$, as

$$[\mathcal{U}(\boldsymbol{x})]_i := \begin{cases}
[\boldsymbol{x}]_i - \gamma[\boldsymbol{w}_1]_i & \text{if } [\boldsymbol{x}]_i \geq [\boldsymbol{\delta}]_i + \gamma[\boldsymbol{w}_1]_i; \\
[\boldsymbol{x}]_i + \gamma[\boldsymbol{w}_1]_i & \text{if } [\boldsymbol{x}]_i \leq [\boldsymbol{\delta}]_i - \gamma[\boldsymbol{w}_1]_i; \\
[\boldsymbol{\delta}]_i & \text{otherwise.}
\end{cases}$$

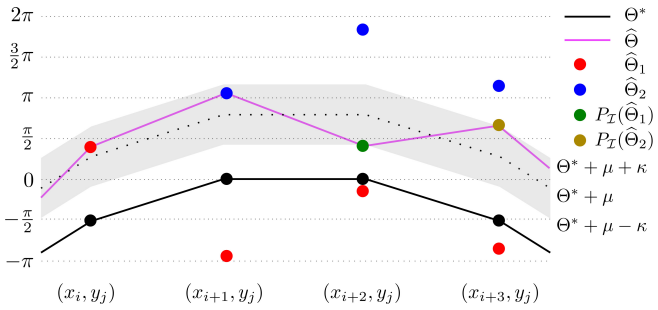

Figure 1: Example of $\widehat{\Theta}$. At (x_i, y_j), $\widehat{\Theta} = \widehat{\Theta}_1$ since $\widehat{\Theta}_1 \in \mathcal{I}$. At (x_{i+1}, y_j), $\widehat{\Theta} = \widehat{\Theta}_2 = \widehat{\Theta}_1 + 2\pi$ since $\widehat{\Theta}_2 \in \mathcal{I}$. At (x_{i+2}, y_j), $\widehat{\Theta} = P_{\mathcal{I}}(\widehat{\Theta}_1) = \Theta^* + \mu - \kappa$ since $\widehat{\Theta}_1, \widehat{\Theta}_2 \notin \mathcal{I}$ and $d(\widehat{\Theta}_1, \mathcal{I}) < d(\widehat{\Theta}_2, \mathcal{I})$. Finally, at (x_{i+3}, y_j), $\widehat{\Theta} = P_{\mathcal{I}}(\widehat{\Theta}_2) = \Theta^* + \mu + \kappa$ since $\widehat{\Theta}_1, \widehat{\Theta}_2 \notin \mathcal{I}$ and $d(\widehat{\Theta}_2, \mathcal{I}) < d(\widehat{\Theta}_1, \mathcal{I})$,

2.2 Inconsistency Correction for Date Fidelity (Step 2)

The minimizer $\boldsymbol{\Theta}^* = \mathrm{vec}(\Theta^*_{i,j})_{j=0,1,\dots,m}^{i=0,1,\dots,n}$ in Step 1 can be seen as a smoothed version of the minimizer of (2) in Section 1. However Θ^* has no guarantee of the consistency $W(\Theta^*_{i,j}) \approx \Theta^W_{i,j}$, which suggests that Θ^* has room for further improvement. In what follows, we carefully construct a corrected version $\widehat{\Theta}$ of Θ^* by noting that a simplest point-wise correction

$$\begin{aligned}\widehat{\Theta}_1(x_i, y_j) &:= \underset{\Theta \text{ s.t. } W(\Theta) = \Theta^W_{i,j}}{\operatorname{argmin}} |\Theta - \Theta^*_{i,j}| \\ &= \Theta^*_{i,j} + W\big(\Theta^W_{i,j} - \Theta^*_{i,j}\big)\end{aligned}$$

easily loses the smoothness of Θ^* (see, e.g., $\widehat{\Theta}_1(x_{i+1}, y_j) - \widehat{\Theta}_1(x_i, y_j)$ in Fig. 1).

We propose to search for a best consistent candidate $\widehat{\Theta}_{i,j}$ at each (x_i, y_j) within

$$\mathcal{I}_{i,j} := [\Theta^*_{i,j} + \mu - \kappa, \Theta^*_{i,j} + \mu + \kappa] \subset \mathbb{R},$$

where $\mu := \frac{1}{(m+1)(n+1)} \sum_{i=0}^{n} \sum_{j=0}^{m} W(\Theta^W_{i,j} - \Theta^*_{i,j})$ and $\kappa \in [0, \pi]$ is chosen to specify a possible range of correction. To construct $\widehat{\Theta}_{i,j}$, we also utilize

$$\begin{aligned}\widehat{\Theta}_2(x_i, y_j) &:= \underset{\Theta \text{ s.t. } W(\Theta) = \Theta^W_{i,j} \text{ and } \Theta \neq \widehat{\Theta}_1(x_i, y_j)}{\operatorname{argmin}} |\Theta - \Theta^*_{i,j}| \\ &= \widehat{\Theta}_1(x_i, y_j) - \operatorname{sgn}\big(\widehat{\Theta}_1(x_i, y_j) - \Theta^*_{i,j}\big) 2\pi\end{aligned}$$

as

$$\widehat{\Theta}_{i,j} := \begin{cases} P_{\mathcal{I}_{i,j}}\big(\widehat{\Theta}_1(x_i, y_j)\big) & \text{if } d\big(\widehat{\Theta}_1(x_i, y_j), \mathcal{I}_{i,j}\big) \\ & \quad \le d\big(\widehat{\Theta}_2(x_i, y_j), \mathcal{I}_{i,j}\big); \\ P_{\mathcal{I}_{i,j}}\big(\widehat{\Theta}_2(x_i, y_j)\big) & \text{if } d\big(\widehat{\Theta}_2(x_i, y_j), \mathcal{I}_{i,j}\big) \\ & \quad < d\big(\widehat{\Theta}_1(x_i, y_j), \mathcal{I}_{i,j}\big), \end{cases}$$

where $P_{\mathcal{I}_{i,j}}(\Theta) \in \mathcal{I}_{i,j}$ is uniquely defined as

$$\min_{\vartheta \in \mathcal{I}_{i,j}} |\Theta - \vartheta| = |\Theta - P_{\mathcal{I}_{i,j}}(\Theta)| =: d(\Theta, \mathcal{I}_{i,j}),$$

and especially $P_{\mathcal{I}_{i,j}}(\Theta) = \Theta$ if $\Theta \in \mathcal{I}_{i,j}$. Note that the proposed correction is realized by point-wise computations as illustrated in Fig. 1, and $\widehat{\Theta}$ does not depend on the order of correction. Moreover, if $\widehat{\Theta}_1(x_i, y_j) \in \mathcal{I}_{i,j}$ or $\widehat{\Theta}_2(x_i, y_j) \in \mathcal{I}_{i,j}$, then $W(\widehat{\Theta}_{i,j}) = \Theta^W_{i,j}$ is guaranteed.

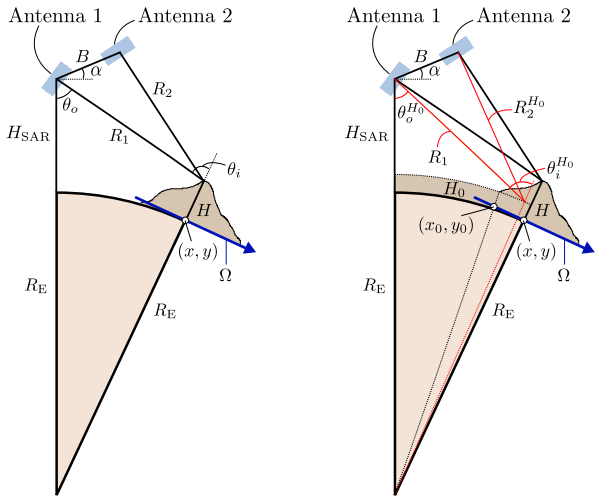

(a) (b)

Figure 2: Outline drawing of terrain height estimation by InSAR. (a) Sectional view for the construction of the interferometric phase. (b) Sectional view for the construction of the reference phase.

3 Application to Terrain Height Estimation

In this section, we apply the proposed 2D phase unwrapping algorithm to terrain height estimation by InSAR.

3.1 Terrain Height Estimation by InSAR

Interferometric synthetic aperture radar (InSAR) [3]–[9] is an imaging technique allowing highly accurate measurements of surface topography in all weather conditions, day or night. In InSAR system (see Fig. 2(a)), Antenna 1 and Antenna 2 on-board an aircraft or a spacecraft platform transmit coherent broadband radio signals and receive the reflected signals $s_k := |s_k| e^{-\imath(\frac{4\pi R_k}{\lambda} + \phi_k + \nu_k)}$ $(k = 1, 2)$ from a target corresponding to $(x, y) \in \Omega \subset \mathbb{R}^2$, where λ is the wavelength of the transmitted signal, R_k is the distance from Antenna k to the target, ϕ_k is the backscatter phase delay, ν_k is additive phase noise, and the dependencies of variables R_k, ϕ_k, ν_k, θ_o and θ_i on (x, y) are omitted for notational simplicity in Fig. 2 and in the discussion below. Since the backscatter phase delay ϕ_k is determined by the shape of the target, geological condition, and weather condition, we can expect $\phi_1 = \phi_2$ in many situations, and hence the interferometric image is obtained as

$$\bar{s}_1 s_2 = |s_1||s_2| e^{\imath(\frac{4\pi(R_1 - R_2)}{\lambda} + \nu)}, \tag{5}$$

where $\bar{s}_1$ denotes the complex conjugate of s_1 and $\nu := \nu_1 - \nu_2$. The *interferometric phase* $\Theta_{\mathrm{int}} := 4\pi(R_1 - R_2)/\lambda$ can also be expressed, from the simple geometric relation in Fig. 2(a) and the law of cosines, as

$$\Theta_{\mathrm{int}} = \frac{4\pi}{\lambda} \left\{ R_1 - \sqrt{R_1^2 + B^2 - 2R_1 B \sin(\theta_o - \alpha)} \right\},$$

and its noisy wrapped samples $\Theta^W_{\mathrm{int}} := W(\Theta_{\mathrm{int}} + \nu)$ are observed from (5).

Suppose that we know the height at (x_0, y_0) as H_0 (see Fig. 2(b)). Then we compute the reference phase $\Theta_{\mathrm{ref}} :=$

$4\pi(R_1 - R_2^{H_0})/\lambda$ expressed as

$$\Theta_{\mathrm{ref}} = \frac{4\pi}{\lambda}\left\{R_1 - \sqrt{R_1^2 + B^2 - 2R_1 B\sin(\theta_o^{H_0} - \alpha)}\right\}$$

s.t. $\cos\theta_o^{H_0} = \frac{R_1^2+(R_{\mathrm{E}}+H_{\mathrm{SAR}})^2-(R_{\mathrm{E}}+H_0)^2}{2R_1(R_{\mathrm{E}}+H_{\mathrm{SAR}})}$, which is a virtual interferometric phase assuming that the terrain height is always H_0. Note that the reference phase can be computed because we can compute $\theta_o^{H_0}$ unlike θ_o. Define the 2D unwrapped phase as $\Theta := \Theta_{\mathrm{int}} - \Theta_{\mathrm{ref}}$. To estimate terrain height H, as a refinement of [30, Equation A.2.3], we newly derive the following relation:

$$\Theta \approx \frac{4\pi B\cos(\theta_o^{H_0} - \alpha)(H - H_0)}{\lambda\sin\theta_i^{H_0}\sqrt{R_1^2 + B^2 - 2R_1 B\sin(\theta_o^{H_0} - \alpha)}}, \quad (6)$$

where $\theta_i^{H_0}$ in Fig. 2(b) is available from $\sin\theta_i^{H_0} = \frac{(R_{\mathrm{E}}+H_{\mathrm{SAR}})\sin\theta_o^{H_0}}{R_{\mathrm{E}}+H_0}$. The noisy wrapped phase $\Theta^W := W(\Theta_{\mathrm{int}} - \Theta_{\mathrm{ref}} + \nu) = W(\Theta_{\mathrm{int}}^W - \Theta_{\mathrm{ref}})$ is obtained from (5) and Θ_{ref}. After reconstructing Θ from Θ^W via 2D phase unwrapping, terrain height H is estimated from (6).

3.2 Numerical Experiments

We demonstrate the effectiveness of the proposed 2D phase unwrapping algorithm by simulation for terrain height estimation based on (6). Figure 3(a) shows the unwrapped phase Θ generated from a mountain shown in Fig. 4(a). Here we set the parameters of InSAR by $\alpha = \pi/6$ [rad], $\lambda = 23.5$ [cm], $B = 500$ [m], $H_{\mathrm{SAR}} = 800$ [km], $R_{\mathrm{E}} = 6371$ [km], $R_1(x_0, y_0) = 1243$ [km], and $H(x_0, y_0) = H_0 = 2530$ [m]. Figure 3(b) depicts the noisy wrapped phase Θ^W observed at regular rectangular grid points $\{(x_i, y_j)\}_{j=0,\ldots,180}^{i=0,\ldots,180}$ on $\Omega := [x_0, x_{180}] \times [y_0, y_{180}]$ s.t. $x_{i+1} - x_i = 16.2$ [m] and $y_{j+1} - y_j = 19.5$ [m]. Figures 3(c), 3(d), 3(e), 3(f), and 3(g) respectively depict the estimates by *branch cut* (BC) [5], *minimum spanning tree* (MST) [26], *minimum cost flow* (MCF) [27], *least squares* (LS) [28], and the propose algorithm with simple parameters ($w_{i,j}^x = w_{i,j}^y = 1$, $w_{i,j}^{xx} = w_{i,j}^{xy} = w_{i,j}^{yy} = 1/100$, $\epsilon = 5 \times 10^{-7}$ and $\kappa = \pi/6$). Figures 4(b), 4(c), 4(d), 4(e) and 4(f) show the mountains constructed from the results in Fig. 3 and (6). From these figures, we find that the proposed algorithm achieves the best performance compared with the other algorithms visually as well as numerically.

Moreover, we obtain the best estimate and mountain as respectively shown in Figs. 3(h) and 4(g), by using the following weights in (4):

$$w_{i,j}^x = \begin{cases} 3 & \text{if } \left|W\left(\Delta_x\Theta_{i,j}^W\right)\right| \in [0, \frac{\pi}{2}]; \\ 6 - \frac{6}{\pi}\left|W\left(\Delta_x\Theta_{i,j}^W\right)\right| & \text{if } \left|W\left(\Delta_x\Theta_{i,j}^W\right)\right| \in (\frac{\pi}{2}, \pi], \end{cases}$$

$$w_{i,j}^y = \begin{cases} 4 & \text{if } \left|W\left(\Delta_y\Theta_{i,j}^W\right)\right| \in [0, \frac{\pi}{2}]; \\ 8 - \frac{8}{\pi}\left|W\left(\Delta_y\Theta_{i,j}^W\right)\right| & \text{if } \left|W\left(\Delta_y\Theta_{i,j}^W\right)\right| \in (\frac{\pi}{2}, \pi], \end{cases}$$

$$w_{i,j}^{xx} = \begin{cases} 1/20 & \text{if } \varphi(i-1, i+3, j-3, j+3) = 1; \\ 1/40 & \text{if } \varphi(i-1, i+3, j-3, j+3) = 0, \end{cases}$$

$$w_{i,j}^{xy} = \begin{cases} 3/40 & \text{if } \varphi(i-2, i+3, j-2, j+3) = 1; \\ 1/40 & \text{if } \varphi(i-2, i+3, j-2, j+3) = 0, \end{cases}$$

and

$$w_{i,j}^{yy} = \begin{cases} 1/10 & \text{if } \varphi(i-3, i+3, j-1, j+3) = 1; \\ 1/40 & \text{if } \varphi(i-3, i+3, j-1, j+3) = 0, \end{cases}$$

where $\Delta_x\Theta_{i,j}^W := \Theta_{i+1,j}^W - \Theta_{i,j}^W$, $\Delta_y\Theta_{i,j}^W := \Theta_{i,j+1}^W - \Theta_{i,j}^W$, and $\varphi : \mathbb{Z}^4 \to \{0, 1\}$ is defined as

$$\varphi(i_{\min}, i_{\max}, j_{\min}, j_{\max}) := \begin{cases} 1 & \text{if } \begin{cases} \text{there exist } \lceil (i_{\max} - i_{\min})(j_{\max} - j_{\min})/3 \rceil \text{ or} \\ \text{more residues in } [x_{i_{\min}}, x_{i_{\max}}] \times [y_{j_{\min}}, y_{j_{\max}}]; \end{cases} \\ 0 & \text{otherwise,} \end{cases}$$

for $0 \le i_{\min} < i_{\max} \le n$ and $0 \le j_{\min} < j_{\max} \le m$ (Note: φ is defined as $\varphi(0, i_{\max}, j_{\min}, j_{\max})$ for $i_{\min} < 0$, $\varphi(i_{\min}, n, j_{\min}, j_{\max})$ for $i_{\max} > n$, $\varphi(i_{\min}, i_{\max}, 0, j_{\max})$ for $j_{\min} < 0$, and $\varphi(i_{\min}, i_{\max}, j_{\min}, m)$ for $j_{\max} > m$). Here we assign larger values to the weights in the y-axis direction by considering the *layover-discontinuity* [31].

Figure 5(a) shows the unwrapped phase Θ based on another mountain in Fig. 6(a). The parameter settings of InSAR and the proposed algorithm are same as those used in the first simulation except $R_1(x_0, y_0) = 1244$ [km] and $H(x_0, y_0) = H_0 = 579$ [m]. Figure 5(b) depicts the noisy wrapped samples Θ^W at grid points $\{(x_i, y_j)\}_{j=0,1\ldots,180}^{i=0,1\ldots,180}$. Figures 5(c), 5(d), 5(e), 5(f), 5(g), and 5(h) respectively depict the estimates by BC, MST, MCF, LS, the proposed algorithm with simple weights, and the proposed algorithm with weights based on the proposed design in Section 2.1.4. Figures 6(b), 6(c), 6(d), 6(e), 6(f) and 6(g) show the mountains constructed from the results in Fig. 5 and (6). The proposed algorithm achieves again the best performance.

4 Conclusion

In this paper, we have proposed a novel 2D phase unwrapping algorithm which is composed of two steps. First, the proposed algorithm computes a minimizer, as a rough estimate of the unwrapped phase, of a newly defined convex cost function. This cost function is designed to enhance smoothness for noisy area as well as to promote data fidelity for the other area. Second, the proposed algorithm corrects the inconsistency between the rough estimate and the observed wrapped sample while keeping a certain level of smoothness. Then this corrected version is used as an estimate of the unwrapped phase. Numerical experiments for terrain height estimation by InSAR showed the effectiveness of the proposed 2D phase unwrapping algorithm.

Acknowledgment

This work was supported in part by JSPS Grants-in-Aid Grant Numbers 26-920 and B-15H02752.

References

[1] D. C. Ghiglia and M. D. Pritt, *Two-Dimensional Phase Unwrapping: Theory, Algorithms, and Software*. New York, NY: Wiley, 1998.

[2] L. Ying, "Phase unwrapping," in *Wiley Encyclopedia of Biomedical Engineering, 6-Volume Set*, M. Akay, Ed. New York, NY: Wiley, 2006.

[3] L. C. Graham, "Synthetic interferometer radar for topographic mapping," *Proceedings of the IEEE*, vol. 62, no. 6, pp. 763–768, Jun. 1974.

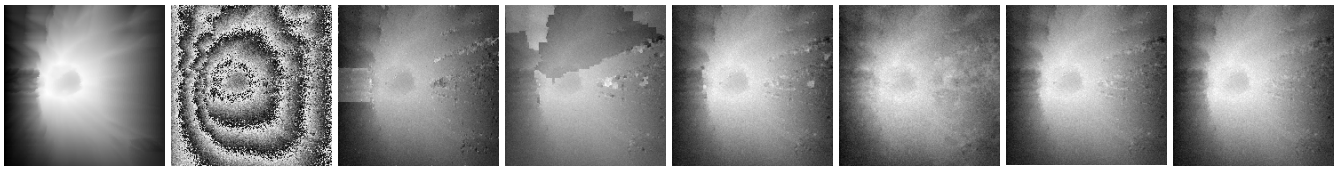

(a) (b) (c) (d) (e) (f) (g) (h)

Figure 3: Estimates $\overline{\Theta}$ of the unwrapped phase Θ from the noisy wrapped phase Θ^W and their mean square errors MSE $:= \frac{1}{32761}\sum_{i=0}^{180}\sum_{j=0}^{180}|\Theta_{i,j}-\overline{\Theta}_{i,j}|^2$. (a) Unwrapped phase Θ. (b) Wrapped phase Θ^W. (c) Estimate by BC (MSE $= 1.7587$). (d) Estimate by MST (MSE $= 8.2192$). (e) Estimate by MCF (MSE $= 0.0974$). (f) Estimate by LS (MSE $= 20.4673$). (g) Estimate by the proposed algorithm with $w^x_{i,j} = w^y_{i,j} = 1$ and $w^{xx}_{i,j} = w^{xy}_{i,j} = w^{yy}_{i,j} = \frac{1}{100}$ (MSE $= 0.0377$). (h) Estimate by the proposed algorithm with wights based on the proposed design (MSE $= 0.0251$).

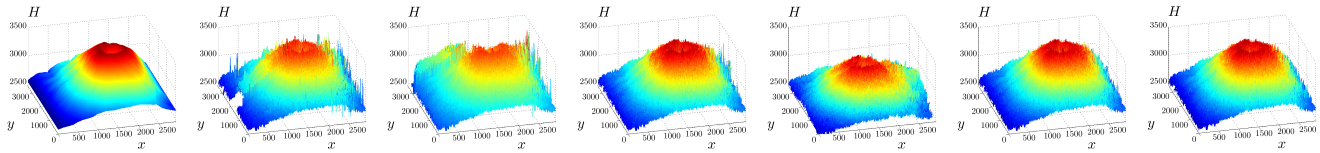

(a) (b) (c) (d) (e) (f) (g)

Figure 4: Estimates $\overline{H}$ of the terrain height H of a mountain based on $\overline{\Theta}$ and (6) and their mean absolute errors MAE $:= \frac{1}{32761}\sum_{i=0}^{180}\sum_{j=0}^{180}|H_{i,j}-\overline{H}_{i,j}|$. (a) Virtual mountain of terrain height H. (b) Estimate by BC (MAE $= 37.6844$). (c) Estimate by MST (MAE $= 87.1949$). (d) Estimate by MCF (MAE $= 26.9321$). (e) Estimate by LS (MAE $= 162.3990$). (f) Estimate by the proposed algorithm with $w^x_{i,j} = w^y_{i,j} = 1$ and $w^{xx}_{i,j} = w^{xy}_{i,j} = w^{yy}_{i,j} = \frac{1}{100}$ (MAE $= 26.0454$). (g) Estimate by the proposed algorithm with wights based on the proposed design (MAE $= 25.6152$).

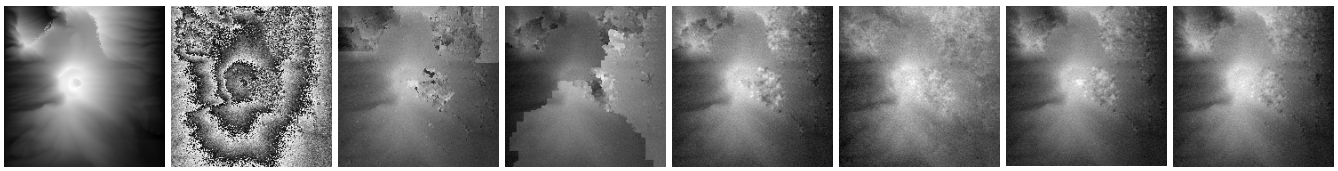

(a) (b) (c) (d) (e) (f) (g) (h)

Figure 5: Estimates $\overline{\Theta}$ of the unwrapped phase Θ from the noisy wrapped phase Θ^W and their mean square errors MSE $:= \frac{1}{32761}\sum_{i=0}^{180}\sum_{j=0}^{180}|\Theta_{i,j}-\overline{\Theta}_{i,j}|^2$. (a) Unwrapped phase Θ. (b) Wrapped phase Θ^W. (c) Estimate by BC (MSE $= 2.5410$). (d) Estimate by MST (MSE $= 49.4547$). (e) Estimate by MCF (MSE $= 1.4087$). (f) Estimate by LS (MSE $= 5.8364$). (g) Estimate by the proposed algorithm with $w^x_{i,j} = w^y_{i,j} = 1$ and $w^{xx}_{i,j} = w^{xy}_{i,j} = w^{yy}_{i,j} = \frac{1}{100}$ (MSE $= 0.1765$). (h) Estimate by the proposed algorithm with wights based on the proposed design (MSE $= 0.1169$).

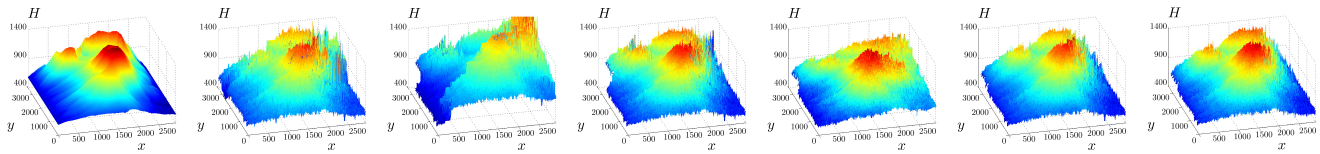

(a) (b) (c) (d) (e) (f) (g)

Figure 6: Estimates $\overline{H}$ of the terrain height H of a mountain based on $\overline{\Theta}$ and (6) and their mean absolute errors MAE $:= \frac{1}{32761}\sum_{i=0}^{180}\sum_{j=0}^{180}|H_{i,j}-\overline{H}_{i,j}|$. (a) Virtual mountain of terrain height H. (b) Estimate by BC (MAE $= 52.1210$). (c) Estimate by MST (MAE $= 210.7460$). (d) Estimate by MCF (MAE $= 41.1130$). (e) Estimate by LS (MAE $= 86.7128$). (f) Estimate by the proposed algorithm with $w^x_{i,j} = w^y_{i,j} = 1$ and $w^{xx}_{i,j} = w^{xy}_{i,j} = w^{yy}_{i,j} = \frac{1}{100}$ (MAE $= 32.9569$). (g) Estimate by the proposed algorithm with wights based on the proposed design (MAE $= 30.6799$).

[4] H. A. Zebker and R. M. Goldstein, "Topographic mapping from interferometric synthetic aperture radar observations," *Journal of Geophysical Research*, vol. 91, no. B5, pp. 4993–4999, Apr. 1986.

[5] R. M. Goldstein, H. A. Zebker, and C. L. Werner, "Satellite radar interferometry: Two-dimensional phase unwrapping," *Radio Science*, vol. 23, no. 4, pp. 713–720, Jul./Aug. 1988.

[6] A. Moccia and S. Vetrella, "A tethered interferometric synthetic aperture radar (SAR) for a topographic mission," *IEEE Transactions on Geoscience and Remote Sensing*, vol. 30, no. 1, pp. 103–109, Jan. 1992.

[7] P. A. Rosen, S. Hensley, I. R. Joughin, F. K. Li, S. N. Madsen, E. Rodriguez, and R. M. Goldstein, "Synthetic aperture radar interferometry," *Proceedings of the IEEE*, vol. 88, no. 3, pp. 333–382, Mar. 2000.

[8] D. Leva, G. Nico, D. Tarchi, J. Fortuny, and A. J. Sieber, "Temporal analysis of a landslide by means of a ground-based SAR interferom-

eter," *IEEE Transactions on Geoscience and Remote Sensing*, vol. 4, no. 4, pp. 745–752, Apr. 2003.

[9] C. Colesanti and J. Wasowski, "Investigating landslides with space-borne synthetic aperture radar (SAR) interferometry," *Engineering Geology*, vol. 88, no. 3–4, pp. 173–199, Dec. 2006.

[10] C. de Moustier and H. Matsumoto, "Seafloor acoustic remote sensing with multibeam echo-sounders and bathymetric sidescan sonar systems," *Marine Geophysical Researchers*, vol. 15, no. 1, pp. 27–42, Jan. 1993.

[11] P. N. Denbigh, "Signal processing strategies for a bathymetric side-scan sonar," *IEEE Journal of Oceanic Engineering*, vol. 19, no. 3, pp. 382–390, Jul. 1994.

[12] R. E. Hansen, T. O. Sæb**o**, K. Gade, and S. Chapman, "Signal processing for AUV based interferometric synthetic aperture sonar," in *Proceedings of MTS/IEEE OCEANS'03*, vol. 5, 2003, pp. 2438–2444.

[13] M. P. Hayes and P. T. Gough, "Synthetic aperture sonar: A review of current status," *IEEE Journal of Oceanic Engineering*, vol. 34, no. 3, pp. 207–224, Jul. 2009.

[14] V. Srinivasan, H. C. Liu, and M. Halioua, "Automated phase-measuring profilometry: a phase mapping approach," *Applied Optics*, vol. 24, no. 2, pp. 185–188, Jan. 1985.

[15] H. Zhao, W. Chen, and Y. Tan, "Phase-unwrapping algorithm for the measurement of three-dimensional object shapes," *Applied Optics*, vol. 33, no. 20, pp. 4497–4500, Jul. 1994.

[16] P. S. Huang, C. Zhang, and F. P. Chiang, "High-speed 3-D shape measurement based on digital fringe projection," *Optical Engineering*, vol. 42, no. 1, pp. 163–168, Jan. 2003.

[17] S. Zhang, "Recent progresses on real-time 3D shape measurement using digital fringe projection techniques," *Optics and Lasers in Engineering*, vol. 48, no. 2, pp. 149–158, Feb. 2010.

[18] P. Cloetens, W. Ludwig, J. Baruchel, D. Van Dyck, J. Van Landuyt, J. P. Guigay, and M. Schlenker, "Holotomography: Quantitative phase tomography with micrometer resolution using hard synchrotron radiation x rays," *Applied Physics Letters*, vol. 75, no. 19, pp. 2912–2914, Nov. 1999.

[19] T. Weitkamp, A. Diaz, C. David, F. Pfeiffer, M. Stampanoni, P. Cloetens, and E. Ziegler, "X-ray phase imaging with a grating interferometer," *Optics Express*, vol. 13, no. 16, pp. 6296–6304, Aug. 2005.

[20] A. Momose, W. Yashiro, Y. Takeda, Y. Suzuki, and T. Hattori, "Phase tomography by X-ray Talbot interferometry for biological imaging," *Japanese Journal of Applied Physics*, vol. 45, no. 6A, pp. 5254–5262, Jun. 2006.

[21] M. Dierolf, A. Menzel, P. Thibault, P. Schneider, C. M. Kewish, R. Wepf, O. Bunk, and F. Pfeiffer, "Ptychographic X-ray computed tomography at the nanoscale," *Nature*, vol. 467, no. 7314, pp. 436–439, Sep. 2010.

[22] G. H. Glover and E. Schneider, "Three-point Dixon technique for true water/fat decomposition with B_0 inhomogeneity correction," *Magnetic Resonance in Medicine*, vol. 18, no. 2, pp. 371–383, Apr. 1991.

[23] J. Szumowski, W. R. Coshow, F. Li, and S. F. Quinn, "Phase unwrapping in the three-point Dixon method for fat suppression MR imaging," *Radiology*, vol. 192, no. 2, pp. 555–561, Aug. 1994.

[24] S. M. Song, S. Napel, N. J. Pelc, and G. H. Glover, "Phase unwrapping of MR phase images using Poisson equation," *IEEE Transactions on Image Processing*, vol. 4, no. 5, pp. 667–676, May 1995.

[25] S. Chaves, Q. S. Xiang, and L. An, "Understanding phase maps in MRI: a new cutline phase unwrapping method," *IEEE Transactions on Medical Imaging*, vol. 21, no. 8, pp. 966–977, Aug. 2002.

[26] C. W. Chen and H. A. Zebker, "Network approaches to two-dimensional phase unwrapping: intractability and two new algorithms," *Journal of the Optical Society of America A: Optics, Image Science, and Vision*, vol. 17, no. 3, pp. 401–414, Mar. 2000.

[27] M. Costantini, "A novel phase unwrapping method based on network programming," *IEEE Transactions on Geoscience and Remote Sensing*, vol. 36, no. 3, pp. 813–821, May 1998.

[28] D. C. Ghiglia and L. A. Romero, "Robust two-dimensional weighted and unweighted phase unwrapping that uses fast transforms and iterative methods," *Journal of the Optical Society of America A: Optics, Image Science, and Vision*, vol. 11, no. 1, pp. 107–117, Jan. 1994.

[29] D. Gabay and B. Mercier, "A dual algorithm for the solution of nonlinear variational problems via finite element approximation," *Computers & Mathematics with Applications*, vol. 2, no. 1, pp. 17–40, 1976.

[30] A. Ferretti, A. Monti-Guarnieri, C. Prati, F. Rocca, and D. Massonnet, *InSAR Principles: Guidelines for SAR Interferometry Processing and Interpretation*, K. Fletcher, Ed. Noordwijk, The Netherlands: ESA Publications, 2007, vol. TM-19.

[31] C. W. Chen and H. A. Zebker, "Two-dimensional phase unwrapping with use of statistical models for cost functions in nonlinear optimization," *Journal of the Optical Society of America A: Optics, Image Science, and Vision*, vol. 18, no. 2, pp. 338–351, Feb. 2001.